

3D Dynamic RTN Simulation of a 25nm MOSFET: The Importance of Variability in Reliability Evaluation of Decananometer Devices

Salvatore Maria Amoroso*, Fikru Adamu-Lema*, Stanislav Markov*, Louis Gerrer* and Asen Asenov*⁺

*Device Modelling Group - University of Glasgow, Glasgow, Scotland, UK
⁺also with Gold Standard Simulations Ltd, Glasgow G12 8QQ, Scotland, UK
 salvatore.amoroso@glasgow.ac.uk

Abstract— In this work we present a 3D dynamic simulation analysis for the reliability evaluation of a decananometer MOSFET device. We have focused our attention on the Random Telegraph Noise (RTN) phenomenon, showing that the statistical variability induced by the discrete nature of matter and charge has a fundamental impact on the reliability performance of nanoscale devices, in both transient and steady-state operating regimes.

Keywords- Random dopants, charge trapping, statistical variability, reliability, RTN, device simulation.

I. INTRODUCTION

Random telegraph noise (RTN) is a rapidly increasing threat to advanced CMOS scaling [1-2]. The impact of RTN on the reliability of SRAM memory cell operation has been shown to be important starting from the 40 nm generation [3] and to be increasing with cell scaling [4-5]. A robust design aiming to RTN threshold voltage instabilities suppression should rely on accurate understanding of the physics governing the RTN phenomenon, including also the interplay with the variability induced by the atomistic nature of dopants [6-7]. Further, the RTN instabilities exhibit significant transient effects when the device is biased under time-dependent gate voltages [8]. In this case, evaluating the reliability by means of a steady-state analysis can lead to misleading results [9]. In this work we present, for the first time, a dynamic RTN simulation study employing a physics-based trapping/detrapping model in presence of atomistic doping. Our analysis shows that variability induced by atomistic doping plays an important role in determining the reliability features of nanoscale devices, both in transient and steady-state conditions. These results advocate the use of 3D statistical simulations as fundamental complement of any experimental characterization of oxide traps leading to RTN.

II. SIMULATION METHODOLOGY

We performed 3D simulations of a well-scaled 25 nm MOSFET device using the GSS ‘atomistic’ simulator GARAND featuring a drift-diffusion approximation with density gradient quantum corrections [10]. Fig.1 shows the

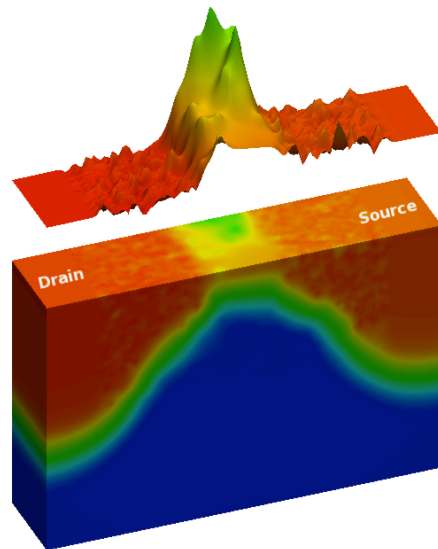


Fig.1 Effective potential for the 25nm atomistic MOSFET ($V_G=0.15V, V_D=0.05V$).

effective potential in the presence of a random configuration of dopants. The single oxide trap leading to RTN is modelled by assigning three positional coordinates (x_T, y_T, z_T) , one energy level $(E_{T,0})$ and a capture cross-section (σ) . In the present study we evaluate the impact of the trap position variability (x_T, y_T) over the channel area, keeping constant $z_T=0.3nm$ (from Si/SiO₂ interface), $\sigma=10^{-14} cm^2$, $E_{T,0}=3.33eV$ (below the SiO₂ conduction band).

Simulation of RTN signal is achieved within a Kinetic Monte Carlo (KMC) engine implemented in GARAND, as shown in Fig.2. After solving the 3D electrostatics and current continuity equation (at $V_G=0.15V, V_D=0.05V$), the average capture time $\langle\tau_c\rangle$ for the single trap is computed integrating the tunnelling gate current density that reaches the trap (WKB approximation) over an area equal to the trap cross-section σ , as explained in [11]. The average emission time $\langle\tau_e\rangle$ is calculated according to the SRH statistics:

$$\frac{\langle\tau_e\rangle}{\langle\tau_c\rangle} = \exp\left(-\frac{E_T - E_{F,n}}{kT}\right) \quad (1)$$

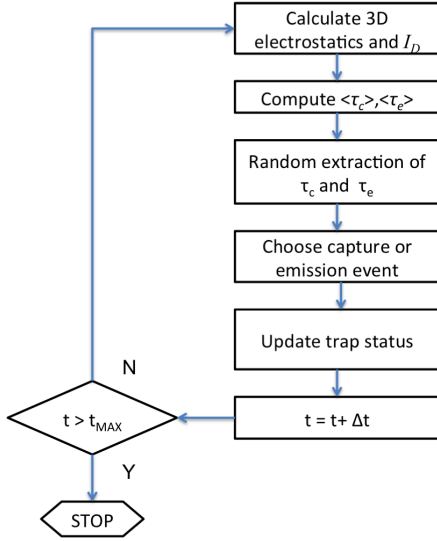


Fig.2 Kinetic Monte Carlo engine for dynamic RTN simulation.

Then the actual capture and emission constants are randomly extracted from exponential distributions of average value $\langle \tau_c \rangle$ and $\langle \tau_e \rangle$. Based on these constants, the KMC-engine choose the next event (capture or emission) and the dynamic simulation time is increased by the extracted τ_c or τ_e . The loop is repeated until the desired reading time is reached. An example of simulated dynamic drain current in presence of a single active RTN trap is presented in Fig.3. Because of the non-negligible trap energy level shift following a trapping event in nanoscale devices (Fig. 4), the SRH statistics may not be fully appropriate for modelling the capture and emission time constants and corrective terms due to Coulomb blockade effects should be taken into account [12]. However, the aim of this work is to stress the importance of variability in reliability simulation of decananometer MOSFETs and not to present an ultimate model for the capture and emission time constants ruling the RTN behaviour.

III. RELIABILITY RESULTS IN PRESENCE OF VARIABILITY

A. RTN time constants and trap occupancy

Figs. 5 and 6 show the dynamic trap occupancy for the two cases studied – continuously doped device and ‘atomistically’ doped device. In both cases the occupancy of the single trap is evaluated for two different trap positions (POS 1 and POS 2 in Fig.7) over the channel area. The trap occupancy, defined as in [9], is obtained by averaging more than 200 dynamic RTN simulations (as Fig. 3) for each case. In the same figures the analytical result obtained from

$$Occ_{in}(t) = Occ_{ss} [1 - \exp(-t / \tau^*)] \quad (2)$$

$$Occ_{ss} = \langle \tau_e \rangle / (\langle \tau_e \rangle + \langle \tau_c \rangle) \quad (3)$$

$$\tau^* = \langle \tau_e \rangle \langle \tau_c \rangle / (\langle \tau_e \rangle + \langle \tau_c \rangle) \quad (4)$$

is also shown, where $\langle \tau_c \rangle$ and $\langle \tau_e \rangle$ are established from the 3D statistical simulations. Note that eqs. (2)-(4) are easily derived assuming that RTN can be described as a Markovian chain, which has been experimentally and analytically demonstrated [13].

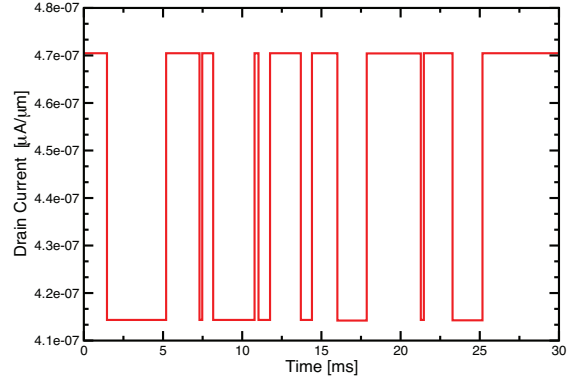


Fig.3 Example of simulated dynamic drain current in presence of a single active RTN trap in the gate oxide.

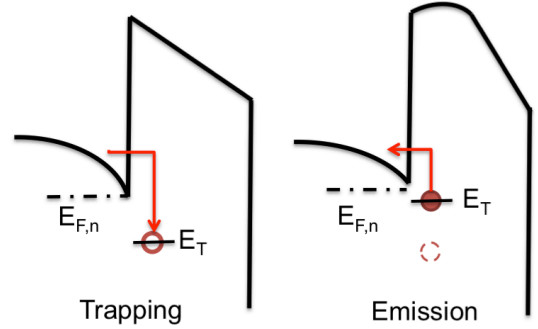


Fig.4 Schematics of the conduction band diagram illustrating trapping and emission process.

Figs. 5 and 6 clearly show the transient effect on the RTN trap occupancy. In particular, erroneous results of reliability performance are obtained for devices operating under dynamic condition with frequency $f > 1/\tau^*$, if trap occupancy is evaluated using a steady-state analysis. Besides, comparison of Fig.5 and Fig.6 demonstrates the critical role played by variability on reliability performance. Indeed, Fig. 6 shows that the RTN behaviour, in both transient and steady-state regime, dramatically changes depending on the trap position over the channel active area. Indeed, not only the steady-state occupancy is different for the two positions in the atomistic device, but also the transient occupancy evolves with completely different time constants (τ^* values are reported in the corresponding pictures captions). Fig. 5 highlights that only a small part of this variability can be attributed to the 3D non-uniform electrostatics over the channel area of a nanoscale transistor. Finally, to generalize this analysis we show in Fig.8 the variability of $\langle \tau_c \rangle$ and $\langle \tau_e \rangle$ due to change of (x_T, y_T) over the whole channel area, emphasizing the impact of the atomistic doping on RTN time constants.

B. RTN power spectral density

The analysis presented in section III.A can be used to study the effects of statistical variability on the RTN power spectrum in the frequency domain. It has been widely assessed that RTN shows a Lorentzian power spectrum with a low frequency plateau followed by a high-frequency tail featuring a $1/f^2$ slope [14-15].

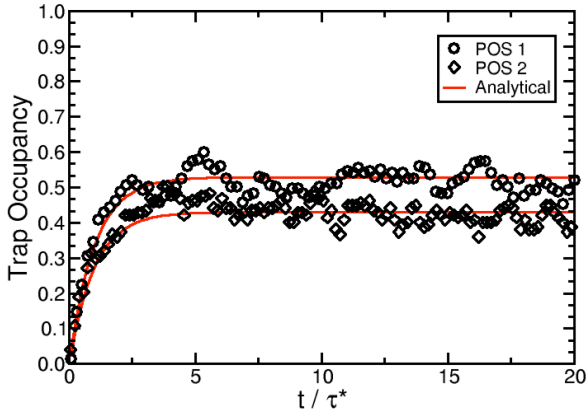


Fig.5 Trap occupancy versus normalized simulation time for the *continuously* doped device in Fig.7. The value of τ^* for the two positions are 1.4×10^{-2} and 1.8×10^{-2} s.

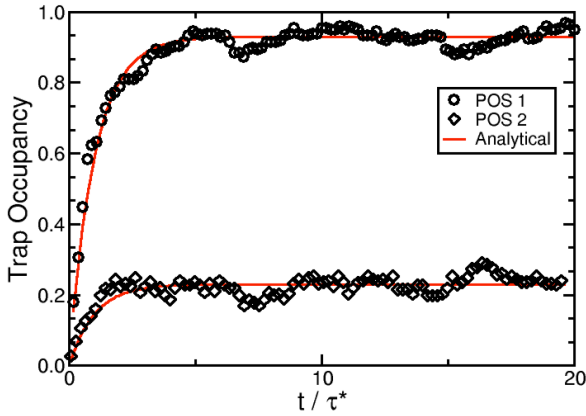


Fig.6 Trap occupancy versus normalized simulation time for the *atomistic* device in Fig.7. The value of τ^* for the two positions are 5.5×10^{-3} and 1.5×10^{-2} s.

Following the Machlup approach [15], the power spectral density of the drain current affected by RTN noise can be written as:

$$S_{I_D}(f) = \frac{4 Occ(1 - Occ) \tau^* \Delta I_D^2}{1 + (2\pi f \tau^*)^2} \quad (5)$$

where f is the frequency, Occ is the trap occupancy probability function as defined in sec. III.A, τ^* is defined by eq. (4) and ΔI_D is the drain current shift following each trapping event (Fig.3). Please note that the occupancy value varies depending whether the gate bias is constant or alternate, as already shown in sec III.A. Moreover, also τ^* assumes different values depending whether the RTN is evaluated under stationary or dynamic gate stress conditions: in the first case τ^* is simply given by eq. (4), while in the second case τ^* needs to be evaluated accordingly to [9]:

$$\frac{1}{\tau^*} = \left(\frac{T_{HIGH}}{T} \right) \frac{1}{\tau_{HIGH}^*} + \left(\frac{T_{LOW}}{T} \right) \frac{1}{\tau_{LOW}^*} \quad (6)$$

where T is the period of the alternate gate bias, T_{HIGH} and T_{LOW} define the duty cycle of the gate signal. Because τ^* strongly depends on the applied gate voltage, then it becomes mandatory to re-evaluate it each time that the applied gate voltage changes: for this reason in eq. (6) we use a different

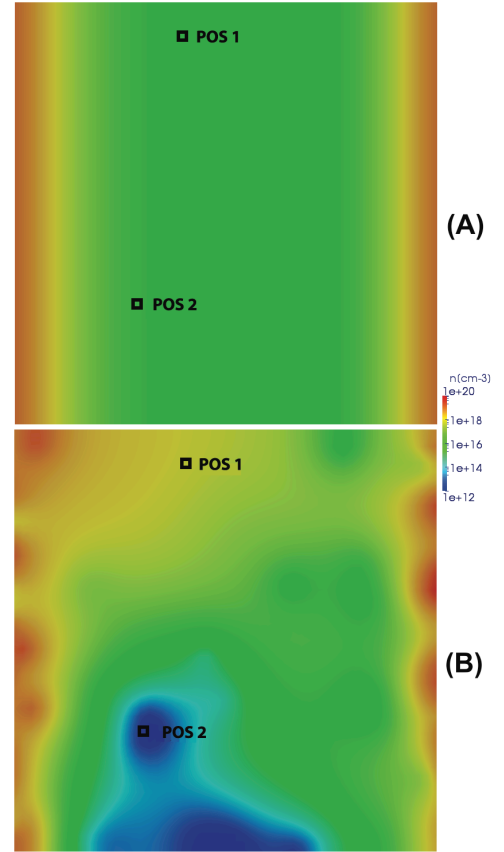


Fig.7 Electron density in the channel area for a *continuously* doped device (A) and an *atomistic* device (B). The two positions of the analyzed trap are also indicated. Traps sketched in figure are unoccupied.

label for τ_{HIGH}^* (τ^* when the gate is high) and for τ_{LOW}^* (τ^* when the gate is low).

Figs. 9 and 10 show the RTN power spectrum for the continuously doped device (see Fig.7A) and for the atomistically doped device (see Fig.7B). It is evident that the noise spectrum is strongly affected by the random dopant fluctuations-induced statistical variability. Further, the effect of applying an alternate gate stress is considered, showing that the noise spectrum can also increase (Fig. 10) and not only decrease when the device is subject to switched bias conditions. This behavior, noticed already in [16], has been experimentally reported [17] and can be captured in simulations only if the τ^* dependence on the applied voltage is taken into account in eq. (6). Please note that, in the case of alternate gate bias, the drain current presents a deterministic alternate behavior that is superimposed to the stochastic RTN signal. The deterministic component results in a series of δ -function peaks in the power spectrum located at f_{switch} , $3f_{switch}$, $5f_{switch}$, etc [16]. These components are not taken into account by eq. (5) and are not of interest for our analysis. Finally, it is worth pointing out that an additional source of variability in the power spectrum comes from the stochastic behavior of ΔI_D . It has been shown that ΔI_D is statistically dispersed over the channel area of a nanoscale device [5,7].

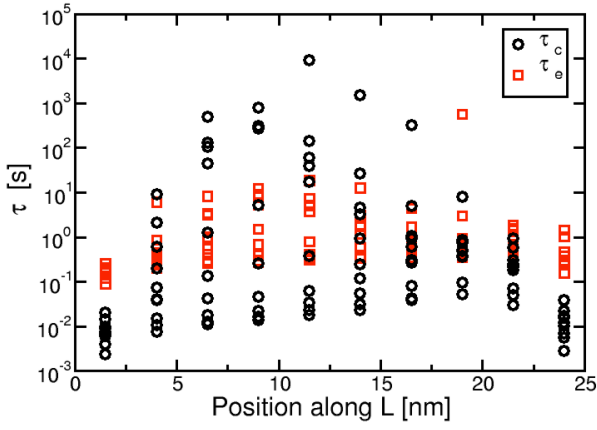


Fig.8 Simulated $\langle\tau_c\rangle$ and $\langle\tau_e\rangle$ as a function of trap position along L for 100 traps uniformly distributed over the channel area (atomistic device in Fig.7).

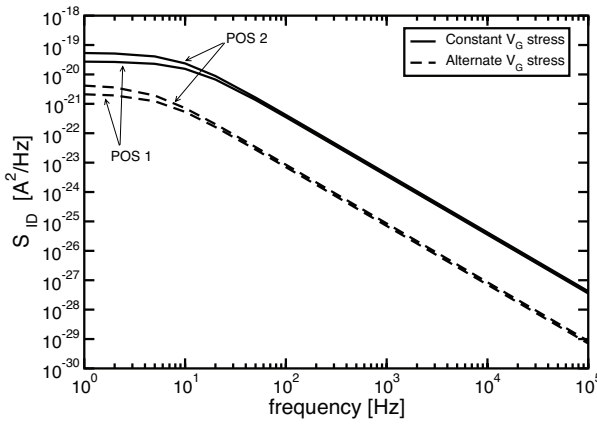


Fig.9 Simulated RTN power spectrum for two trap positions, using a constant (solid lines) and alternate (dashed lines, $f_{\text{switch}}=1\text{kHz}$, duty cycle 50%) gate stress. Continuously doped device in Fig.7.

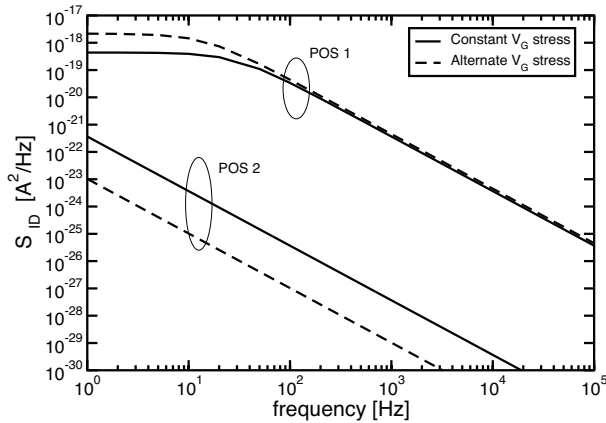


Fig.10 Simulated RTN power spectrum for two trap positions, using a constant (solid lines) and alternate (dashed lines, $f_{\text{switch}}=1\text{kHz}$, duty cycle 50%) gate stress. Atomistically doped device in Fig.7.

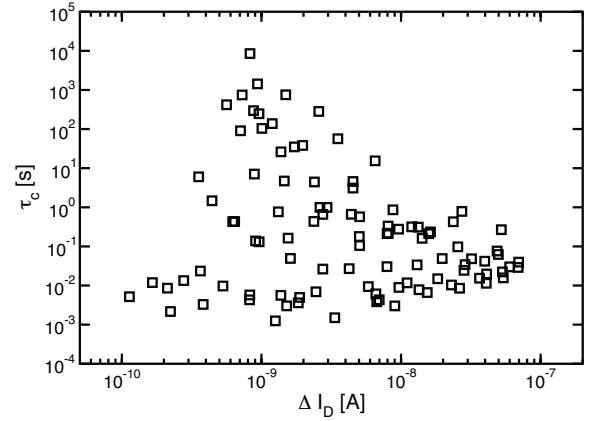


Fig.11 Simulated $\langle\tau_c\rangle$ as a function of ΔI_D for 100 trap positions uniformly distributed over the channel area (atomistic device in Fig.7).

We show in Fig.11 that not only ΔI_D is statistically dispersed over the channel area, but also that ΔI_D and τ_c^* are totally uncorrelated, making it clear that the power spectrum density cannot completely characterize the corresponding RTN in nanoscale devices.

IV. CONCLUSIONS

We have presented for the first time a 3D dynamic simulation analysis of the RTN related reliability behaviour of decananometer MOSFETs. We have shown that variability due to atomistic doping is of utmost importance in assessing the static and transient RTN behaviour and its impact on the reliability performance of nanoscale transistors.

ACKNOWLEDGMENT

This work has received funding from the *MORDRED* project (EU Project 261868).

REFERENCES

- [1] T. Nagumo *et al.*, IEDM 2010, pp.628-631.
- [2] J.P. Campbell *et al.*, IRPS 2009, pp.382-388.
- [3] K. Takeuchi *et al.*, VLSI 2010, pp.189-190.
- [4] N. Tega *et al.*, VLSI 2009, pp.50-51.
- [5] A. Ghetti *et al.*, IEDM 2008, pp.1-4.
- [6] A. Mauri *et al.*, IEDM 2011, pp.405-408.
- [7] A. Asenov *et al.*, Trans. Elec. Dev., pp.839- 845 (2003).
- [8] B. Dierickx *et al.*, J. Appl. Phys., pp.2028- 2029 (1992).
- [9] J. S. Kolhatkar *et al.*, IEDM 2004, pp.759-762.
- [10] <http://www.goldstandardsimulations.com>
- [11] S. M. Amoroso *et al.*, IEDM 2010, pp.540-543.
- [12] A. Palma *et al.*, Phys. Rev. B, pp. 9565–9574 (1997).
- [13] C. M. Compagnoni *et al.*, Trans. Elec. Dev., pp.388-395 (2008).
- [14] M. J. Kirton *et al.*, Adv. Phys., pp.367-468 (1989).
- [15] S. Machlup, J. Appl. Phys., 341-343 (1954).
- [16] A. P. van der Wel *et al.*, Trans. Elec. Dev., pp.1378-1384 (2003).
- [17] A. P. van der Wel *et al.*, Elec. Dev. Lett., pp.56-57 (2001).